Journal of Ceramic Processing Research. Vol. 17, No. 8, pp. 881~884 (2016)

J O U R N A L O F
Ceramic Processing Research

Dielectric and thermal properties of Na_2O-CaO-SiO_2-MgO-Al_2O_3-TiO_2 glass-ceramic

Omer Kaygili*, Fahrettin Yakuphanoglu and Cengiz Tatar
Department of Physics, Faculty of Science, Firat University, Elazig 23119, Turkey

The Na_2O-CaO-SiO_2-MgO-Al_2O_3-TiO_2 (NCSMAT) glass-ceramic having the composition of 49 Na_2O, 19 CaO, 31 SiO_2, 0.25 MgO, 0.50 Al_2O_3 and 0.25 TiO_2 (wt.%) was prepared by conventional method. The crystal structure, phase composition, microstructural, chemical, thermal and dielectric properties of the glass-ceramic were investigated. Using the X-ray diffraction (XRD) results, biphasic structure of the glass-ceramic sample was detected, the crystallite size was found to be 13.21 nm for $Na_4CaSi_3O_9$ phase and 11.02 nm for $Na_8Al_4Si_4O_{18}$ phase, and the crystallinity percent was calculated to be 86.74 %. Scanning electron microscope (SEM) observations show that the NCSMAT glass-ceramic has the fine-grained particle distribution with the smaller particles than 1 μm. The stretching modes of Si-O-Si bound were detected from Fourier transform infrared (FTIR) spectrum. The NCSMAT glass-ceramic is thermally stable from room temperature to 1173 K and the mass loss of the sample in this range is 1.05%. The density was calculated to be 2,751 kg m^{-3}. The relative permittivity at 1 kHz was found to be 85.35. The alternating current conductivity increases with increasing frequency and obeys the universal power law.

Key words: Glass-ceramic, Crystal structure, Thermal stability, Dielectric properties.

Introduction

Glass-ceramics, which are fine-grained and polycrystalline materials, have been produced through the controlled crystallization process of the base glass after nucleation and extremely used for various purposes in many different industrial applications including glass-wares, fire resistant plates, security windows, oven and cook panels [1-5]. There are lots of glass-ceramic types such as Na_2O-CaO-SiO_2 (NCS), Li_2O-Al_2O_3-SiO_2 (LAS), MgO-Al_2O_3-SiO_2 (MAS), CaO-Al_2O_3-SiO_2 (CAS) and Na_2O-PbO-SiO_2 [6-12]. Among these, the NCS based glass-ceramics have been still investigated because of a great importance in the glass industry [13]. Fujibayashi *et al.* [14] studied the apatite forming ability of the P_2O_5-free NCS glass in simulated body fluid (SBF). Harizanova *et al.* [15] investigated the effect of the addition of Fe_2O_3, ranging from 5 to 20 mol % on the electrical conductivity of the NCS glasses. A study related to the effect of TiO_2 addition, within the range from 0 to 10 wt.%, on the crystallization kinetics of a NCS glass was reported by de la Parra-Arciniega *et al.* [16]. As mentioned above, the use of the glass-ceramics in medical applications has got a great importance, and the Na_2O-CaO-P_2O_5-SiO_2 based special glass-ceramic materials have been still produced for this aim [17, 18]. Recently, a phosphate-free NCS based glass-ceramic sample, having biocompatibility and antibacterial activity, has been successfully prepared by Cabal *et al.* [19]. Based on the positive results of the aforementioned article, we produced a new phosphate-free NCS based glass-ceramic sample with the chemical composition of Na_2O-CaO-SiO_2-MgO-Al_2O_3-TiO_2 (NCSMAT). The chemical structure, morphology and dielectric properties of the NCSMAT glass-ceramic sample were investigated to obtain the detailed information about the NCS glass-ceramic system. In terms of being a guide for future works related to the use of the NCSMAT glass-ceramic system for biomedical applications, the present study has been offered a detailed report on the structural properties of this sample.

*Corresponding author:
Tel : +90-424-2370000 / 3623
Fax: +90-424-2330062l
E-mail: okaygili@firat.edu.tr

Experimental Procedures

Na_2CO_3, CaO, SiO_2, MgO, Al_2O_3 and TiO_2 were obtained from Merck and used without any purification. The preparation process of the glass-ceramic sample is as given below. All the powders with the composition of 49 Na_2O, 19 CaO, 31 SiO_2, 0.25 MgO, 0.50 Al_2O_3 and 0.25 TiO_2 (wt.%) were mixed mechanically for 1.5 hrs to ensure homogeneity and gradually heated and melted in an electrical furnace at 1473 K in a platinum crucible. The melted glass was heat treated at 1023 K for 7 hrs, quenched into cold water and dried at 393 K temperature for about 8 hrs.

To investigate the crystal structure and phase composition of the glass-ceramic sample, X-ray diffraction (XRD) analysis was performed using a Bruker D8 Advance diffractometer operated at 40 kV and 40 mA using a Cu Ká radiation with the wavelength of 0.15406 nm. The crystalline phases are matched with the Joint Committee on Powder Diffraction Standards (JCPDS) cards. The lattice parameters ($a = b = c$) for both phases were

calculated using the formula belonging to cubic crystal structure. Using the well-known Debye-Scherrer equation, the crystallite size (D) of the glass-ceramic was calculated [20]:

$$D = \frac{0.9\lambda}{B_{1/2}\cos\theta} \quad (1)$$

where λ is the wavelength of the X-rays and is equals to the value of 0.15406 nm for CuKá radiation, $B_{1/2}$ is the full width at half maximum (FWHM) in radian and θ is the diffraction angle in degree. The crystallinity percent (X_C%) was estimated by the following relation [21]:

$$X_C\% = \frac{\sum A_C}{\sum A_C + \sum A_A} \times 100 \quad (2)$$

where $\sum A_C$ is the total area under crystal peaks, and $\sum A_A$ is the total area under amorphous peaks.

Using the KBr pellet, Fourier transform infrared (FTIR) spectrum was recorded by a PerkinElmer Spectrum One Spectrometer in the range of 400-4000 cm^{-1} at 4 cm^{-1} resolution.

The density (ρ_s) of the glass-ceramic sample was calculated by the following Archimedes method [22]:

$$\rho_s = \frac{W_a}{W_a - W_b} \times \rho_l \quad (3)$$

where W_a and W_l are weights of the sample in air and liquid, respectively. ρ_l is the density of the immersion liquid. The glass-ceramic sample was immersed in distilled water to calculate its density, and this measurement was repeated three times.

Differential thermal analysis (DTA) and thermogravimetric (TG) analysis measurements were carried out using differential thermal analyzer (DTA-50, Shimadzu) and thermogravimetric analyzer (TGA-50, Shimadzu) at heating rate of 10 K min^{-1} from room temperature to 1173 K.

The dielectric study was carried out using a HIOKI 3532-50 LCR HiTESTER at room temperature. Using the measured values of the capacitance (C) of the sample with the thickness of l and effective area of A, the relative permittivity (ε') can be calculated by the following relation [23]:

$$\varepsilon' = \frac{C \times l}{\varepsilon_o \times A} \quad (4)$$

where ε_o is the permittivity of free space. To determine the conductivity mechanism, the well-known Jonscher relation [24] can be used

$$\sigma_{ac} = \sigma_{dc} + B\omega^s \quad (5)$$

where σ_{dc} is the direct current conductivity, B is a constant, ω is the angular frequency and s is the power law exponent lying in the range $0 < s < 1$. The s value is calculated from the slope of $\log\sigma_{ac}$ vs. $\log\omega$ plot.

The morphology was investigated by scanning electron microscope (SEM, JEOL JSM 7001F) at an operating voltage of 30 kV.

Results and Discussion

XRD pattern of the glass-ceramic sample shown in Fig. 1 exhibits the narrow and sharp peaks, indicating a high crystalline structure. Two different phases with cubic crystal structure were observed. The first one is $Na_4CaSi_3O_9$ (sodium calcium silicate, PDF No: 37-0282) and the second one is $Na_8Al_4Si_4O_{18}$ (sodium aluminum silicate, PDF No: 72-1386). The XRD data were evaluated using the XPowder software [25]. For the dominant phase observed on the XRD pattern, the lattice parameter was calculated to be $a = 1.5081$ nm and is in agreement with the reported value ($a = 1.5104$ nm) for $Na_4CaSi_3O_9$ (PDF No: 37-0282). The lattice parameter belonging to the secondary phase of $Na_8Al_4Si_4O_{18}$ was estimated to be $a = 0.7270$ nm and is equal to the standard value of $a = 0.7270$ nm (PDF No: 72-1386).

The average crystallite size values for $Na_4CaSi_3O_9$ and $Na_8Al_4Si_4O_{18}$ crystalline phases were computed to be 13.21 nm and 11.02 nm, respectively. Both values are approximately half of the reported value (25.14 nm) for the NCS glass-ceramic [22]. This difference may be due to the different heat treatment procedure and/or extra additives such as MgO, Al_2O_3 and TiO_2.

The crystallinity percent of the glass-ceramic sample was calculated to be 86.74 %. This result is a perfect harmony with the values for two different NCS glass-ceramics reported by Lu *et al.* [26]. The high crystallinity may be associated with the high amount of Na_2O, which has the improving effects on the crystallization mechanism, and heat treatment [27].

SEM micrographs of the NCSMAT glass-ceramic sample at the magnifications of X 1000, X 2000, X 5000 and X 10000 are shown in Fig. 2. The NCSMAT

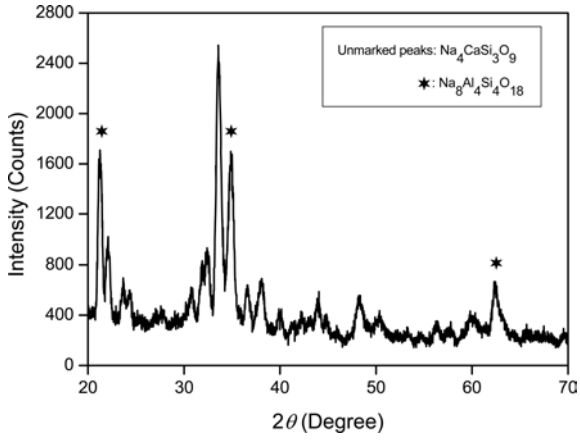

Fig. 1. XRD pattern of the NCSMAT glass-ceramic sample.

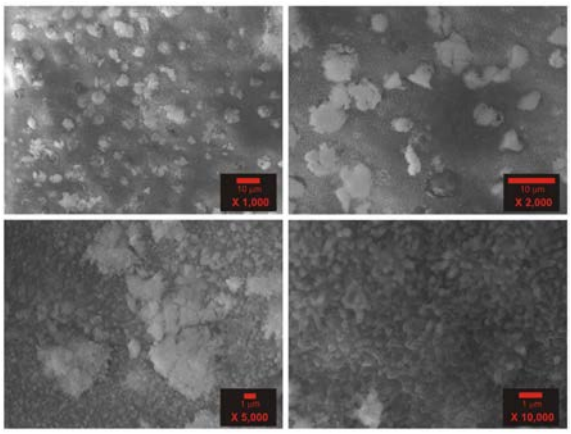

Fig. 2. SEM images of the sample at various magnifications.

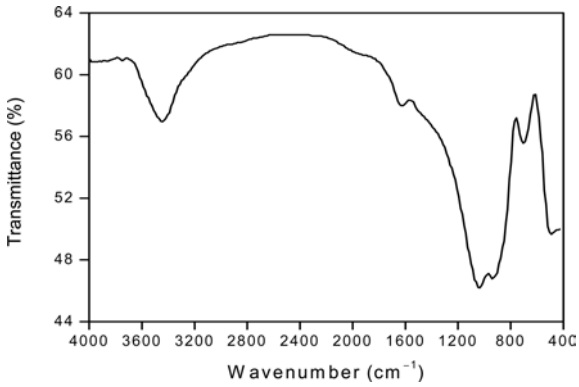

Fig. 3. FTIR spectrum of the NCSMAT glass-ceramic sample.

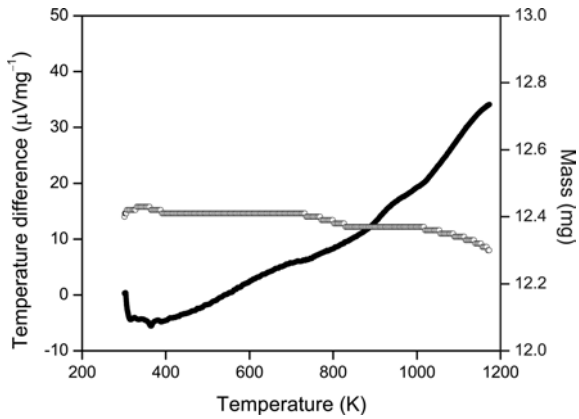

Fig. 4. DTA and TG curves of the NCSMAT glass-ceramic sample from room temperature to 1173 K.

sample exhibits the fine-grained and aggregated structure. The particle sizes are smaller than that of the value of 1 μm and this is in good agreement with the literature [1, 22].

FTIR spectrum of the NCSMAT glass-ceramic is shown in Fig. 3. The bands at 3437 and 1631 cm^{-1} are related to the absorbed water, and the other bands at 1036, 922, and 688 cm^{-1} are assigned to the stretching modes of Si-O-Si bound [28-32].

Fig. 4 shows the DTA and TG plots of the as-prepared sample in the temperature from room temperature to

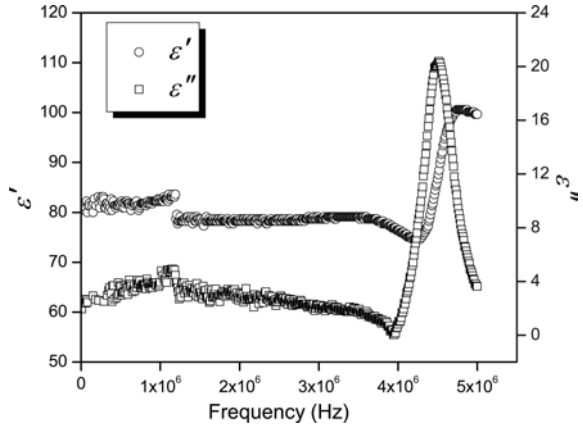

Fig. 5. The plots of relative permittivity and dielectric loss as a function of frequency.

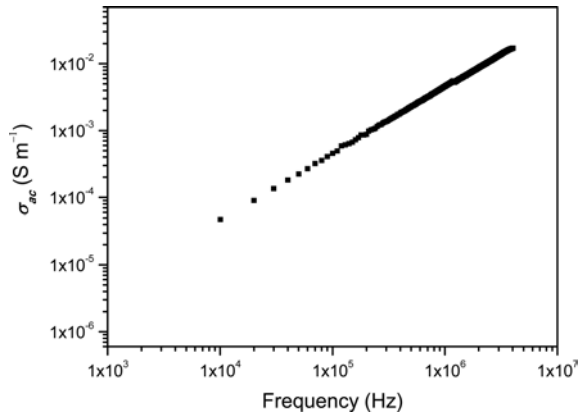

Fig. 6. The alternating current conductivity as a function of frequency plot of the NCSMAT glass-ceramic.

1173 K. Compared to the NCS glass-ceramic, the NCSMAT sample has a high thermal stability. Although the thermal behavior of the as prepared NCS glass-ceramic is similar to the NCS based bioactive glass-ceramic (BGC) until about 973 K, at higher temperatures the NCS glass-ceramic is more stable than that of the NCS based BGC. While the mass loss of the NCS based BGC is about 28%, this loss is equal to the value of 1.05% for the NCS glass-ceramic in the range from room temperature to 1173 K [33].

The mean value of density was calculated to be 2,751 kg m^{-3}. This is so close to the theoretical value (2,778 kg m^{-3}) for $Na_4CaSi_3O_9$ (PDF No: 37-0282). Moreover, this value is in accordance with the reported values for both the NCS glass-ceramic and the NCS based bioactive glasses in the literature [22, 34].

The ε' values at 1 kHz, 100 kHz, 500 kHz, 2 MHz and 4 MHz were found to be 85.35, 81.78, 81.33, 78.65 and 76.42, respectively. The ε' value of the NCSMAT at 1 kHz is close to the reported value (94.44) for the MAS glass-ceramic [35]. Fig. 5 shows the plots of the relative permittivity (ε') and dielectric loss (ε''), which calculated from the loss tangent (tan δ) times ε' values, as a function of frequency.

Both parameters show the decreasing tendency with increasing frequency until about 4 MHz. Beyond this frequency value, a relaxation peak was observed at about 4.5 MHz. This peak may be associated to dipolar or electronic polarization mechanism of the sample [36].

As shown in Fig. 6, the alternating current conductivity (σ_{ac}) of the NCSMAT glass-ceramic increases with the increasing frequency. The increase of the alternating current conductivity with increasing frequency obeys the universal power law behavior. The value of power law exponent (s) is calculated to be 0.9956 and is equal to unity. This result means that the hopping motion involves a translational motion with a sudden hopping [37, 38].

Conclusions

The NCSMAT glass-ceramic was produced by the conventional melting technique after heat treatment process at 1023 K for 7 hrs. The crystalline phases of $Na_4CaSi_3O_9$ and $Na_8Al_4Si_4O_{18}$ with cubic crystal structure were observed. The average crystallite size values were estimated to be 13.21 nm for $Na_4CaSi_3O_9$ phase and 11.02 nm for $Na_8Al_4Si_4O_{18}$ phase. Additionally, the crystallinity percent was computed to be 86.74%. The stretching modes belonging to the Si-O-Si bound were detected. From room temperature to 1173 K, the NCSMAT glass-ceramic is thermally stable, and the mass loss is found to be 1.05 % in the same temperature range. The density calculated from the Archimedes method is 2,751 kg m^{-3}. The relative permittivity at 1 kHz was found to be 85.35. With the increasing frequency, the relative permittivity and dielectric loss vary. The alternating current conductivity increases almost linearly with increasing frequency and obeys the universal power law. The NCSMAT glass-ceramic has the fine-grained particle distribution with the smaller particles than 1 μm.

References

1. P.W. McMillan, “Glass-Ceramics” (Academic Press, 1979).
2. H.R. Fernandes, D.U. Tulyaganov, and J.M.F. Ferreira, J. Therm. Anal. Calorim. 112[3] (2013) 1359-1368.
3. J. Holubová, Z. Černošek, and E. Černošková, J. Therm. Anal. Calorim. 114[3] (2013) 997-1002.
4. O. Kaygili, and H. Yavuz, J. Therm. Anal. Calorim. 102[2] (2010) 681-684.
5. W. Holland, G. Beall, “Glass-Ceramic Technology” (The American Ceramic Society, 2002).
6. V.M. Fokin, and E.D. Zanotto, J. Non-Cryst. Solids 353 [24-25] (2007) 2459-2468.
7. T. Berthier, V.M. Fokin, and E.D. Zanotto, J. Non-Cryst. Solids 354[15-16] (2008) 1721-1730.
8. Y. Li, K. Liang, B. Xu, and J.W. Cao, J. Therm. Anal. Calorim. 101[3] (2010) 941-948.
9. M. Goswami, A. Sarkar, B.I. Sharma, V.K. Shrikhande, and G.P. Kothiyal, J. Therm. Anal. Calorim. 78[3] (2004) 699-705.
10. H. Li, J. Cheng, and L. Tang, J. Non-Cryst. Solids 354[12-13] (2008) 1418-1423.
11. O.C. Mocioiu, M. Zaharescu, I. Atkinson, A.M. Mocioiu, and P. Budrugeac, J. Therm. Anal. Calorim. 117[1] (2014) 131-139.
12. M. Reben, and M. Œroda, J. Therm. Anal. Calorim. 113[1] (2013) 77-81.
13. Z. Zhang, Y. Xiao, J. Voncken, Y. Yang, R. Boom, N. Wang, and Z. Zou, J. Am. Ceram. Soc. 94[9] (2011) 3088-3093.
14. S. Fujibayashi, M. Neo, H.M. Kim, T. Kokubo, and T. Nakamura, Biomaterials 24[8] (2003) 1349-1356.
15. R. Harizanova, R. Keding, and C. Rüssel, J. Non-Cryst. Solids 354[1] (2008) 65-71.
16. S.M. de la Parra-Arciniega, A. Álvarez-Méndez, L.C. Torres-González, and E.M. Sánchez, Rev. Mex. Fis. 55[1] (2009) 32-37.
17. B. Mirhadia, and B. Mehdikhanib, New Journal of Glass and Ceramics 2 (2012) 1-6.
18. L.L. Hench, D.E. Day, W. Höland, and V.M. Rheinberger, Int. J. Appl. Glass Sci. 1[1] (2010) 104-117.
19. B. Cabal, L. Alou, F. Cafini, R. Couceiro, D. Sevillano, L. Esteban-Tejeda, F. Guitian, R. Torrecillas, and J.S. Moya, Sci. Rep. 4 (2014) 1-9.
20. B.D. Cullity, “Elements of X-ray diffraction” (Addison-Wesley Publishing Company, 1978).
21. O. Kaygili, S. Keser, T. Ates, and F. Yakuphanoglu, Ceram. Int. 39[7] (2013) 7779-7785.
22. O. Kaygili, J. Therm. Anal. Calorim. 117[1] (2014) 223-227.
23. N. Sivakumar, N. Kanagathara, K. Gayatri, P. Krishnan, and G. Anbalagan, J. Therm. Anal. Calorim. 115[2] (2014) 1295-1301.
24. A.K. Jonscher, Nature 267 (1977) 673-679.
25. J.D. Martin, Using XPowder: A software package for Powder X-Ray diffraction analysis. www.xpowder.com, D.L. GR 1001/04.ISBN 84-609-1497-6. 2004, 105 p. Spain.
26. A. Lu, X. Hu, Y. Lei, Z. Luo, and X. Li, Ceram. Int. 40[1] (2014) 11-16.
27. J. Cao, and Z. Wang, J. Alloys Compd. 557 (2013) 190-195.
28. H.A. ElBatal, M.A. Azooz, E.M.A. Khalil, A.S. Monem, and Y.M. Hamdy, Mater. Chem. Phys. 80[3] (2003) 599-609.
29. O.P. Filho, G.P. LaTorre, and L.L. Hench, J. Biomed. Mater. Res. Part A30[4] (1998) 509-514.
30. F.H. ElBatal, and A. ElKheshen, Mater. Chem. Phys. 110[2-3] (2008) 352-362.
31. F. Branda, A. Costantini, G. Luciani, and G. Laudisio, J. Therm. Anal. Calorim. 64[3] (2001) 1017-1024.
32. M. Sitarz, W. Mozgawa, and M. Handke, J. Mol. Struct. 511-512 (1999) 281-285.
33. R.L. Siqueira, and E.D. Zanotto, Mater. Sci. Eng. C 31[8] (2011) 1791-1799.
34. H. Doweidar, J. Non-Cryst. Solids 355[9] (2009) 577-580.
35. A. Prasad, and A. Basu, Journal of Advanced Ceramics 2 [1] (2013) 71-78.
36. M.S. Jogad, B.S. Krishnamurthy, G.P. Kothiyal, and V. Saraswati, Current Science 83[9] (2002) 1121-1124.
37. J.C. Dyre, and T.B. Schrøder, Rev. Mod. Phys. 72[3] (2000) 873-892.
38. K. Funke, Prog. Solid State Chem. 22[2] (1993) 111-195.